*metals*

MDPI

*Article*

# A Study on Friction Stir Processing Parameters of Recycled AA 6063/$TiO_2$ Surface Composites for Better Tribological Performance

**Guo Sheng Teo, Kia Wai Liew * and Chee Kuang Kok**

SIG-Machine Design and Tribology, Centre for Advanced Mechanical and Green Technology, Faculty of Engineering and Technology, Multimedia University, Jalan Ayer Keroh Lama, Melaka 75450, Malaysia

* Correspondence: kwliew@mmu.edu.my or mscalec@gmail.com; Tel.: +60-606-252-3507

**Abstract:** This work aims to determine and select the suitable friction stir processing parameters for recycled aluminum alloy 6063 surface composites reinforced with titanium dioxide for better tribological performance. A medium range of processing parameters (1200–2000 rpm, 25–45 mm/min) were used to compare with a unique relatively high rotational speed of 2442 rpm and feed rate of 50 mm/min for the sample fabrication. The surface composites' microhardness was measured and the friction and wear performance were tested using the pin-on-disc tribo-tester under starved lubrication conditions. The results show that surface composites produced at a high rotational speed of 2442 rpm and feed rate of 50 mm/min improved 45% in surface microhardness and reduced the friction coefficient and wear rate by 39% and 73%, respectively, compared to the substrate material.

**Keywords:** friction stir processing (FSP); FSP parameters selection; FSPed recycled AA 6063/$TiO_2$ surface composites; surface microhardness; tribological performance



**Citation:** Teo, G.S.; Liew, K.W.; Kok, C.K. A Study on Friction Stir Processing Parameters of Recycled AA 6063/$TiO_2$ Surface Composites for Better Tribological Performance. *Metals* **2022**, *12*, 973. https://doi.org/10.3390/met12060973

Academic Editors: Young-Sik Pyun, Do-Sik Shim and Evgeny A. Kolubaev

Received: 25 April 2022
Accepted: 31 May 2022
Published: 6 June 2022



## 1. Introduction

Surface engineering is an essential engineering technique that is used for a wide range of applications as it has led to significant energy savings, especially for tribological applications [1]. In tribological applications, the surface properties are more essential than the bulk material properties [2]. Hence, material surface properties used in tribological applications are always emphasized. Surface composites can enhance the surface properties while remaining as the base material properties [3]. Friction stir processing (FSP) is a surface engineering approach that can be used for surface composite fabrication [3] and is energy-efficient and environmentally friendly [4–6]. FSP was developed from friction stir welding (FSW) by The Welding Institute (TWI) in the year 1991 [7]. Three different FSP methods can be used for surface composite fabrication: groove method, cover-plate method and drill-holes method [3,8,9]. The fabrication of surface composites via FSP requires two different types of tools: the capping tool and the friction stir tool. The capping tool is used for sealing the reinforcement particles, while the friction stir tool is used to mix the reinforcement particles into the surface metal matrix [3].

The selection of FSP parameters is very important to produce surface composites with desired performance, especially the rotational speed and feed rates, as they control major heat generation during FSP [3]. According to previous FSP works [10–14], different processing parameters were reported for FSPed aluminum alloy 6063 (AA 6063). In this study, the FSP parameters that can produce the best tribological performance and surface microhardness for FSPed recycled AA 6063 surface composites, reinforced with titanium dioxide ($TiO_2$), will be determined.

$TiO_2$ is an environmentally friendly and stable component that has been utilized in many industries [15,16]. Heidarpour et al. [17], who studied Cu/$TiO_2$ surface composites

that had been friction stir processed, reported that $TiO_2$ can enhance the surface hardness of the substrate material. This improvement in surface hardness also contributed to the enhancement of tribological performance for the substrate material. On the other hand, Khodabakhshi et al. [18] have reported that $TiO_2$ nano-powder has improved surface hardness, yield strength and tensile strength of AA 5052 substrate material. Meanwhile, Abraham J.S. et al. [19] have also reported that $TiO_2$ particles have excellent bonding with AA 6063 matrix after being put through FSP to form surface composites. However, there is still limited information about the tribological performance of the aluminum alloy surface composites reinforced with $TiO_2$ using FSP. Hence, $TiO_2$ was selected as the reinforcement particles to use in FSP of recycled AA 6063/$TiO_2$ surface composites in this study.

In short, there has been limited study on the tribological performance of FSP of AA 6063/$TiO_2$. Furthermore, different FSP parameters were used in the previous studies for aluminum alloy surface composites materials. Therefore, the aim of this work is to select suitable FSP parameters for the fabrication of FSPed recycled AA 6063/$TiO_2$ to improve the tribological performance of recycled AA 6063 substrate material. The process parameters for FSP in this study are derived from the author's previous work [10].

## 2. Materials and Methods

### *2.1. Substrate Material and Reinforcement Particles*

Recycled AA 6063 was selected as a substrate material in this study. The chemical composition of the substrate material is shown in Table 1. The substrate material was prepared in the shape of a rectangular bar with dimensions of 175 × 36 × 25 $mm^3$ (L × W × H). Titanium dioxide ($TiO_2$) nano-powder, having an average particle size of 21 nm, was obtained from Sigma Aldrich as the selected reinforcement particles. Figure 1 shows the photograph of $TiO_2$ nano-powder.

**Table 1.** Chemical composition (wt.%) of recycled AA 6063.

| Element | Zn | Mg | Cu | Si | Fe | Mn | Cr | Ni | Ti | Al |
|---|---|---|---|---|---|---|---|---|---|---|
| wt.% | 0.0331 | 0.581 | 0.0338 | 0.43 | 0.309 | 0.0252 | 0.0335 | 0.0333 | 0.0269 | Balance |

**Figure 1.** Photograph of $TiO_2$ Nano-powder.

### *2.2. Groove Cutting and Reinforcement Particles Allocation*

The groove FSP method was used in this study. It is the most common type of FSP method used to produce aluminum surface composites. A groove with dimensions of (135 × 3 × 2) $mm^3$ (L × W × D) was cut as a reservoir to allocate the reinforcement particles, using the CNC Milling Machine, Mazak, Japan. Next, the mass of the $TiO_2$ nano-powder (0.2 g) was measured using an electronics balance to ensure the $TiO_2$ nano-powder integration into each workpiece was consistent. Figure 2 shows the $TiO_2$ nano-powder inserted in the groove on the recycled AA 6063 substrate material.

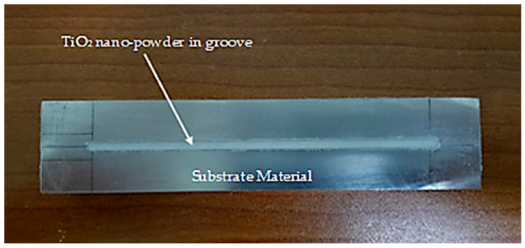


**Figure 2.** $TiO_2$ inserted in the groove on the substrate material.

### *2.3. Capping Process*

The capping process was conducted using a pin-less FSP tool that was attached to a manual milling machine. A rotational speed of 1600 rpm and feed rate of 80 mm/min were used to seal up the $TiO_2$ nano-powder in the groove. The capping depth was set to 0.3 mm. The schematic diagram of capping is presented in Figure 3. The pin-less FSP tool was made by ASP 23 high-speed steel.

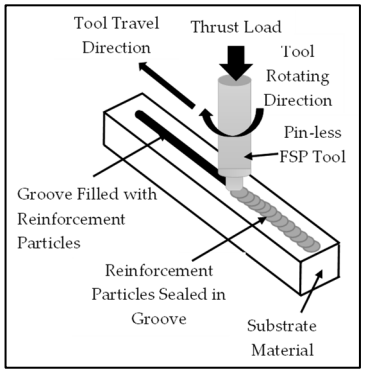


**Figure 3.** Schematic diagram of capping.

### *2.4. Friction Stir Processing (FSP)*

Figure 4a shows the schematic diagram of FSP. A taper threaded FSP tool, which was made with ASP 23 high-speed steel with a tool shoulder diameter of 18 mm, a tapered probe length of 5 mm, and a major and minor diameter of 7 mm and 5 mm, respectively, was used for the FSPed sample fabrication. The FSP was conducted using the CNC Milling Machine, Mazak, Japan. Table 2 shows the lists of FSP parameters that were used for the fabrication of FSPed recycled AA 6063/$TiO_2$ surface composites. The rotational speeds and feed rates were selected based on the relatively low friction coefficient, or wear rate, of FSPed recycled AA 6063, garnered from the authors' previous work [10]. However, increase in rotational speed might ensure a better distribution of reinforcement particles in the surface metal matrix [20]. In addition, a higher rotational speed with a lower feed rate could attain a homogeneous distribution of reinforcement particles in the surface metal matrix [21]. On the other hand, the un-treated recycled AA 6063 that was used in the current work would easily deform, due to the excessive heat generated during FSP when rotational speed exceeding 2500 rpm with low feed rate was applied. Hence, a unique rotational speed of 2442 rpm, with a feed rate of 50 mm/min, was intentionally and rationally selected from the relatively high rotational speed range (2400–2500 rpm) to compare with the selected processing parameters at the varied medium speed range (1200–2000 rpm) and feed rate (25–45 mm/min) used in this study. The FSP ploughing depth was set to 0.5 mm. The photograph of FSPed recycled AA 6063/$TiO_2$ surface composites is shown in Figure 4b.

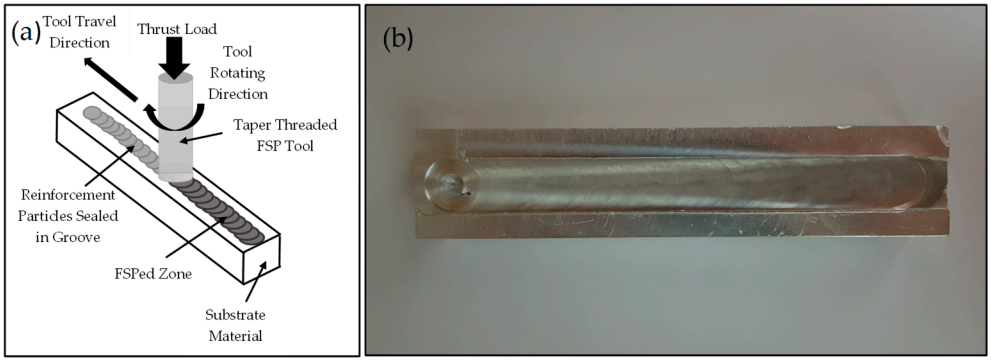


**Figure 4.** (**a**) Schematic diagram of friction stir processing and (**b**) FSPed recycled AA 6063/$TiO_2$ surface produced at 2442 rpm and 50 mm/min.

**Table 2.** FSP parameters used for the fabrication of FSPed recycled AA 6063/$TiO_2$ surface composites samples.

| Sample | Processing Parameters | |
|---|---|---|
| | **Rotational Speed (rpm)** | **Feed Rate (mm/min)** |
| 1200-30 | 1200 | 30 |
| 1200-35 | 1200 | 35 |
| 1400-25 | 1400 | 25 |
| 1400-30 | 1400 | 30 |
| 1600-30 | 1600 | 30 |
| 1600-35 | 1600 | 35 |
| 1600-40 | 1600 | 40 |
| 1600-45 | 1600 | 45 |
| 1800-35 | 1800 | 35 |
| 1800-40 | 1800 | 40 |
| 1800-45 | 1800 | 45 |
| 2000-25 | 2000 | 25 |
| 2000-35 | 2000 | 35 |
| 2000-40 | 2000 | 40 |
| 2442-50 | 2442 | 50 |

### *2.5. Surface Roughness Measurement*

The surface roughness produced by different processing parameters of FSP was measured using the MarSurf M400 C (Mahr, Göttingen, Germany). The effect of rotational speeds and feed rates on surface roughness were analyzed.

### *2.6. Microstructure Analysis*

Microstructure and surface microhardness samples of the substrate material and the FSPed workpieces were cut with dimensions of (36 × 20 × 15) $mm^3$ (W × L × H). Figure 5a demonstrates the sample cutting from the FSPed workpiece and Figure 5b shows the image of the sample (before grinding and polishing). The samples were ground using water-proof silicon carbide papers and polished with diamond paste loaded with colloidal silica until the surfaces became a mirror finish. The grinding and polishing were done using the Forcipol 2V grinding and polishing machine, Metkon, Alaşarköy, Turkey. All polished samples were etched using Keller's reagent before microstructure observation. The microstructure of FSPed samples were observed using a scanning electron microscope

(Hitachi, Tokyo, Japan) and metallurgical microscope (Meiji, Saitama, Japan). The grain size of the samples was measured using VIS Pro software, as demonstrated in Figure 6.

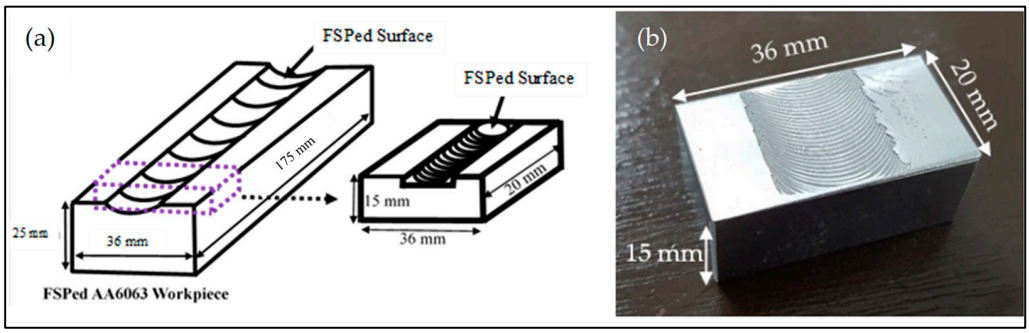


**Figure 5.** (**a**) Demonstration of test sample cut from the FSPed workpiece [10] and (**b**) actual image for microstructure and surface microhardness sample.

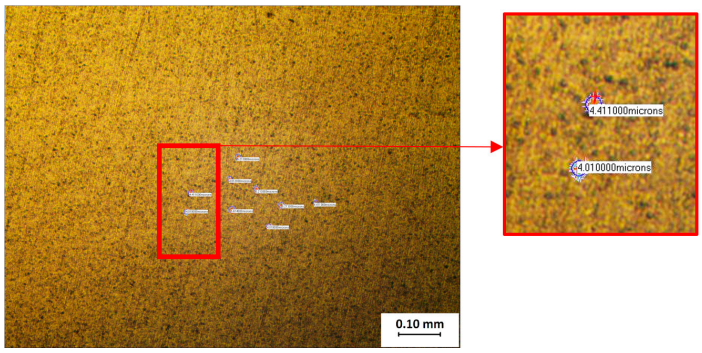


**Figure 6.** Demonstration of grain size measurement.

### *2.7. Surface Microhardness Measurement*

The surface microhardness of the substrate material and the FSPed samples produced by different processing parameters were measured using the Wilson 430 SVD Vickers Hardness Tester (Buehler, Lake Bluff, IL, USA) with a load of 9.81 N and dwell time of 10 s. The samples were ground and polished prior to microhardness measurement. Thirteen indentations were taken in a straight line along the width of the stir zone at the top of the FSPed sample surface and the location of each indentation taken was labelled from −6 to 6.

### *2.8. Friction and Wear Tests*

The friction and wear performance of the substrate material and the FSPed samples produced by different processing parameters were tested using the pin-on-disc tribo-tester under starved lubrication conditions. Distilled water was used as the lubricant and slowly dropped onto the counter disc with a minimum flow rate, using a burette, to simulate starved lubrication conditions during the tests. S275 JR shipbuilding steel was selected as the counter disc surface. Tribo-test pins with dimensions of (11 × 11 × 20) $mm^3$ (L × W × H) were cut from the substrate and FSPed workpieces. Figure 7a demonstrates the pin specimen cut from the FSPed workpiece and Figure 7b shows the actual image of the square tribo-test pin with the ground FSPed surface. In this study, the tribo-test pin was tested in varying speeds, nominal contact pressures and sliding distances. Table 3 shows the detailed parameters for the tribo-tests.

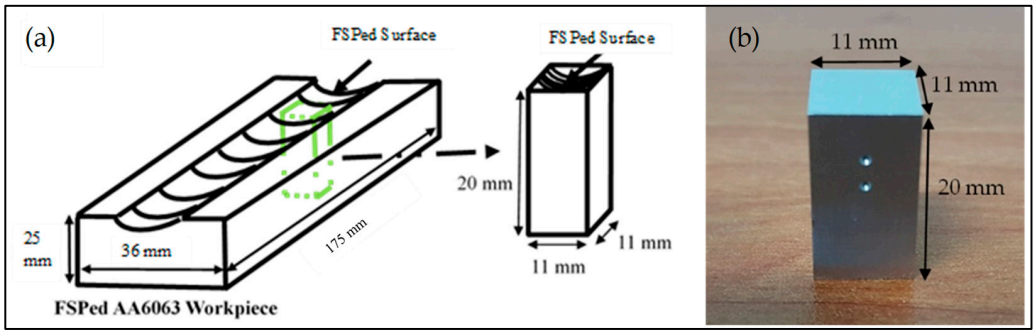


**Figure 7.** (**a**) Demonstration of test sample cut from the FSPed Workpiece [10] and (**b**) actual image for tribo-test pin.

**Table 3.** Tribo-tests parameters.

| Tribo-Tests | Parameters |
| --- | --- |
| **Varying nominal contact pressures** | Nominal contact pressures: 0.08 MPa, 0.16 MPa, 0.24 MPa, 0.32 MPa, 0.41 MPa, 0.47 MPa<br>Speed: 5.18 m/s<br>Sliding duration: 120 s |
| **Varying speeds** | Speeds: 1 m/s, 2 m/s, 3 m/s, 4 m/s, 5 m/s, 6 m/s<br>Nominal contact pressure: 0.28 MPa<br>Sliding duration: 120 s |
| **Varying sliding distances** | Sliding distance: 2.5 km<br>Speed: 2.88 m/s<br>Nominal contact pressure: 0.24 MPa |

## 3. Results and Discussion

### *3.1. Microstructure Analysis*

Grain refinement and several zones, i.e., stir zone, thermo-mechanical affected zone and heat-affected zone, from the FSPed recycled AA 6063/$TiO_2$ samples were discovered and viewed, with results similar to those with FSPed recycled AA6063 from the authors' previous work [10]. Hence, the microstructure analysis in the current work is merely focused on the samples' stir zones. Figure 8 presents the intersection of the stir zone, the-mechanical affected zone and the heat-affected zone under 5× magnification, while Figure 9 shows all the stir zone microstructure of the FSPed recycled AA 6063/$TiO_2$ produced by different processing parameters under 50× magnifications. The thermo-mechanical affected zone shows the oriented grain structure, which was formed according to the shearing direction of the tool shoulder [10]. Grain refinement could also be observed in the thermo-mechanical affected zone. The heat-affected zone is similar to the base metal, with a slight grain refinement [10]. The stir zone microstructures show some black dots, which are the $TiO_2$ nano-powder particles reinforced with the aluminum matrix. This can be justified by comparing the microstructure of the FSPed recycled AA 6063 sample and the SEM images, as shown in Figures 10 and 11. Figures 10a and 11a show additional black dots and white portions in the microstructure and the SEM images that do not exist in Figures 10b and 11b. This proves the successful incorporation of $TiO_2$ into the aluminum matrix. The amount of $TiO_2$ (0.2 g, 20 vol.%) that was incorporated into the aluminum matrix was the same for different FSP processing parameters. However, the microstructure shows that the sample produced at 2442 rpm and 50 mm/min (2442-50) has the most homogeneous distribution of $TiO_2$ among all the samples. In addition, the microstructures also show small grain sizes at the stir zones.

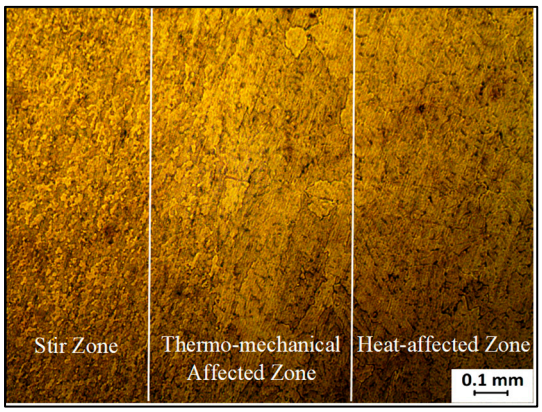


**Figure 8.** Microstructure of stir zone, thermo-mechanical affected zone, and heat-affected zone (5×) of FSPed recycled AA 6063/$TiO_2$ surface composites.

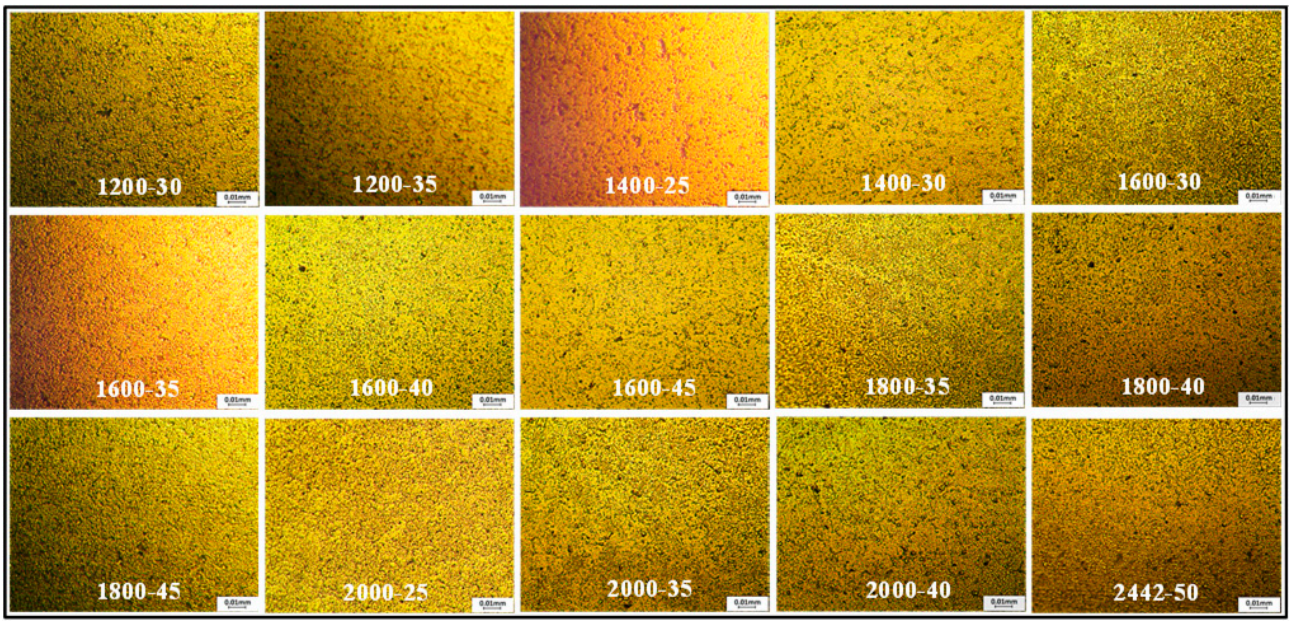


**Figure 9.** Stir zone microstructures (50×) for FSPed recycled AA 6063/$TiO_2$ produced by different processing parameters.

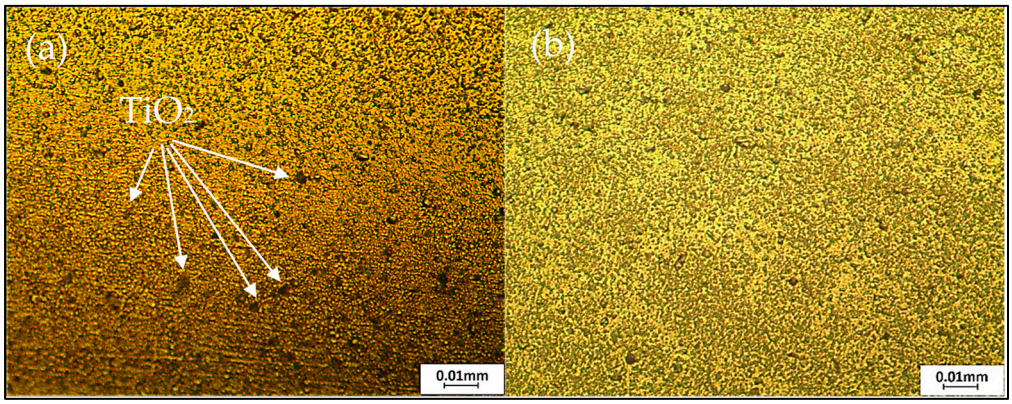


**Figure 10.** Microstructures (50×) of (**a**) FSPed recycled AA 6063/$TiO_2$ and (**b**) FSPed recycled AA 6063 produced at 2442 rpm and 50 mm/min.

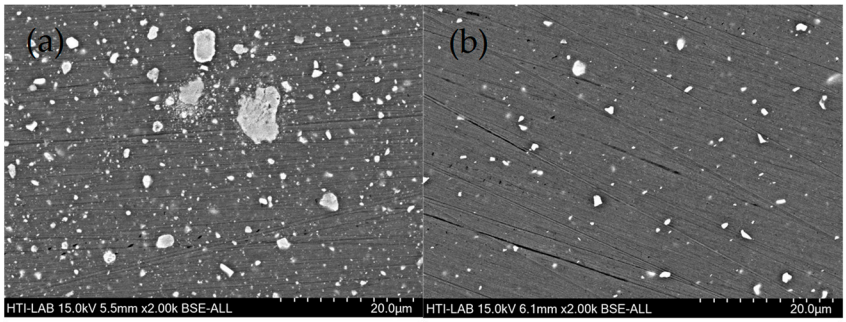


**Figure 11.** SEM Images of (2000×) (**a**) FSPed recycled AA 6063/$TiO_2$ and (**b**) FSPed recycled AA 6063 produced at 2442 rpm and 50 mm/min.

The grain sizes of all the FSPed samples at the stir zone, produced by different processing parameters, were also measured and the result is presented in Figure 12. The results show that the stir zone experienced the greatest reductions in grain size, followed by the thermo-mechanical affected zone and heat-affected zone. Meanwhile, the substrate remained the largest grain size. The stir zone grain sizes are within the range of 5.7 µm to 13 µm. The smallest grain size is achieved by the samples produced at 1200 rpm and 30 mm/min and at 2442 rpm and 50 mm/min, which is about 5.7 µm. In addition, the thermo-mechanical affected zone grain size ranged from 17 µm to 35 µm, while the heat-affected zone has an average grain size ranging from 44 µm to 86 µm. Lastly, the unprocessed base metal zone remained the largest grain size; more than 92 µm. This result shows that FSP led to grain refinement and the existence of $TiO_2$ nano-powder prevented the occurrence of grain growth. Similar findings of grain refinement and pitting effect preventing grain growth, resulting from the incorporation of reinforcement particles in FSP, were also reported by Qin et al. [22].

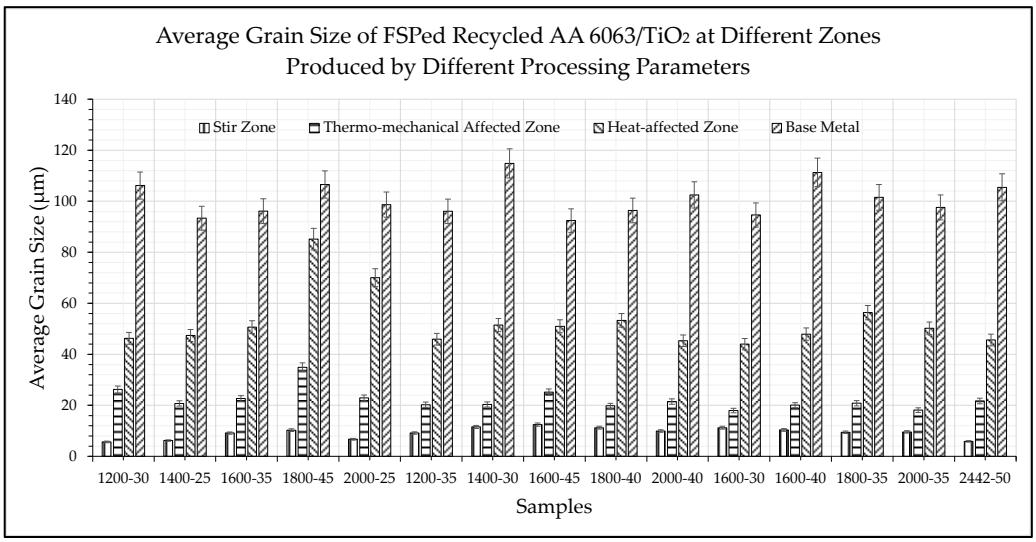


**Figure 12.** The average grain size of FSPed samples at different zones produced by different processing parameters.

### *3.2. Microhardness Measurement*

The average surface microhardness of the substrate material and the FSPed samples are presented in Figure 13. A comparison of the average stir zone microhardness of FSPed recycled AA 6063/$TiO_2$ with FSPed recycled AA 6063 is shown in Figure 14. Figures 13 and 14 show that all the FSPed samples have very similar surface microhardness and the average stir zone microhardness is between 50 HV1 to 56 HV1, as the amount of $TiO_2$ reinforced with the substrate was the same. However, the different processing param-

eters resulted in different distribution of $TiO_2$ particles in FSPed recycled AA 6063/$TiO_2$ surface composites and, hence, led to variation in surface microhardness. In Figure 13, the FSPed sample, produced at 2442 rpm and 50 mm/min (red line), shows the most consistent surface microhardness in the stir zone due to the sample having the most uniform distribution of $TiO_2$ particles. The evidence for uniform distribution of $TiO_2$ nano-powder can be observed in the SEM micrograph, shown in Figure 11a. Figure 14 also shows that all the FSPed recycled AA 6063/$TiO_2$ have higher average surface microhardness at the stir zone than the FSPed recycled AA 6063. The FSP parameters of 1200 rpm with 30 mm/min, 1800 rpm with 45 mm/min, and 2442 rpm with 50 mm/min that were used to produce FSPed recycled AA 6063 have the same surface microhardness (48 HV1). However, the highest average stir zone microhardness (55.96 HV1) is only achieved by the FSPed recycled AA 6063/$TiO_2$ sample, produced at 2442 rpm and 50 mm/min. This shows that higher rotational speed is needed to achieve uniform distribution of the $TiO_2$ reinforcement particles in FSPed recycled AA 6063/$TiO_2$ surface composites. As compared to previous FSPed AA 6063/$TiO_2$ work [19], where the AA 6063 was heat-treated material and, hence, enhancement in surface microhardness was much higher than in this work. However, the enhancement in surface microhardness in this study is also considerably high, as the substrate used in this study was the material without any treatment.

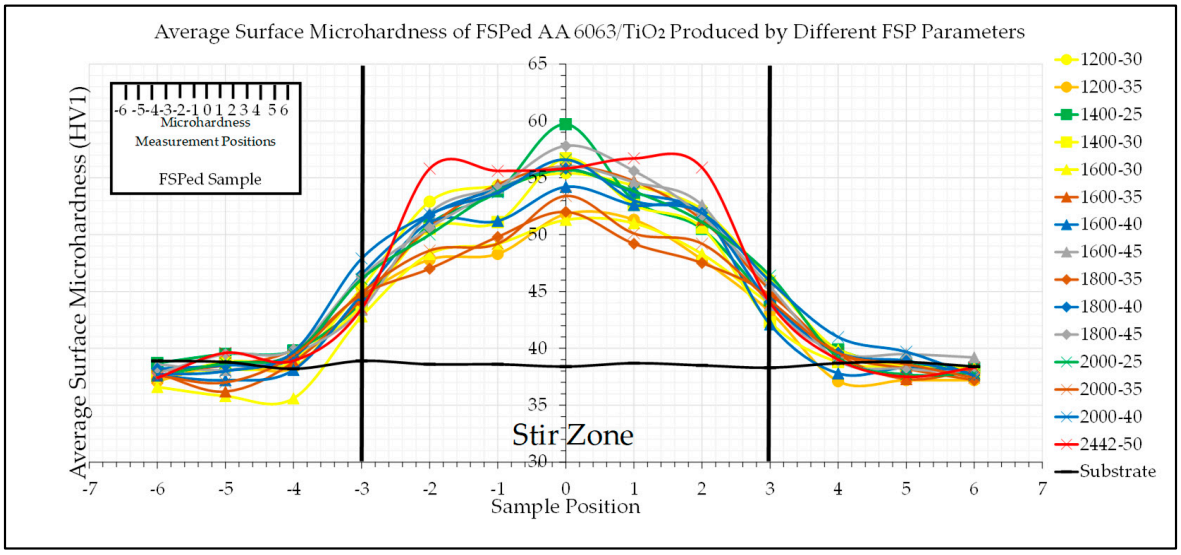


**Figure 13.** Average surface microhardness of substrate material and FSPed recycled AA 6063/$TiO_2$ produced by different processing parameters.

The surface microhardness results show that the incorporation of $TiO_2$ nano-powder further improved the surface microhardness of FSPed recycled AA 6063 and a higher rotational speed is important to ensure uniform distribution of the reinforcement particles. Besides these findings, enhancement of surface microhardness is also caused by grain refinement [19,23].

### *3.3. Surface Roughness Measurement*

The FSPed recycled AA 6063/$TiO_2$ surface roughness, compared with the FSPed recycled AA 6063 is presented in Figure 14. Figure 15a,b show that most of the FSPed recycled AA 6063/$TiO_2$ have lower $R_a$ and $R_q$ values than the FSPed recycled AA 6063. except the sample produced at 1200 rpm and 35 mm/min. The reduction of $R_a$ and $R_q$ values may be due to the incorporation of $TiO_2$ which reduced microscopic peaks and valleys on the surfaces. The increase in $R_a$ value may be due to non-homogeneous distribution of $TiO_2$. Figure 15c,d also show that the $R_{sk}$ and $R_{ku}$ of FSPed recycled AA

6063/$TiO_2$ are more than in the FSPed recycled AA 6063, which is also attributed to the reinforcement of $TiO_2$ sharpening the onion rings during FSP.

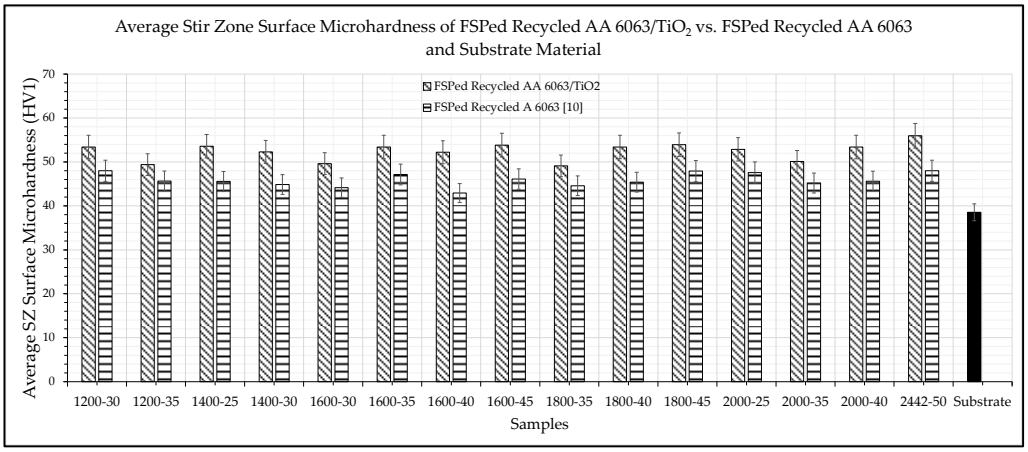


**Figure 14.** Stir zone microhardness of FSPed recycled AA 6063/$TiO_2$ vs. FSPed recycled AA 6063 and substrate material.

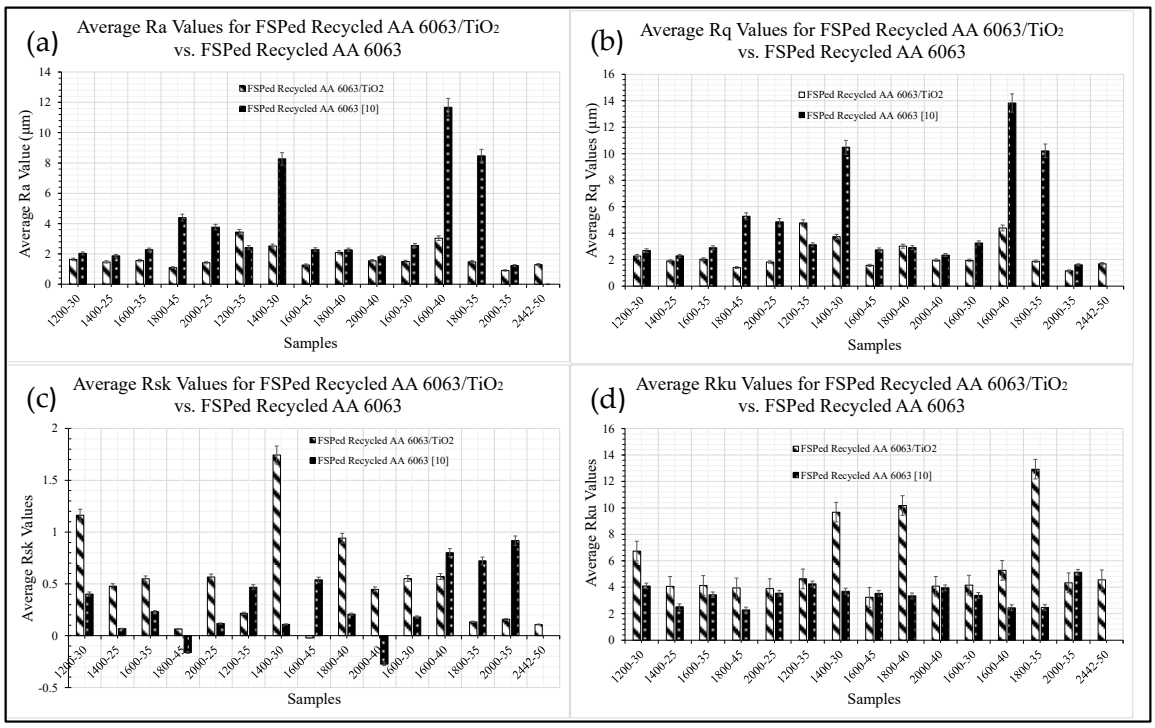


**Figure 15.** Surface roughness of FSPed recycled AA 6063/$TiO_2$ produced by selected processing parameters as compared to FSPed recycled AA6063.

### *3.4. Tribological Performance*

The friction and wear performance of FSPed recycled AA 6063/$TiO_2$ were tested for varying nominal contact pressures, sliding speeds and sliding distances under starved lubrication conditions. The results are presented in Figures 16–20. Figure 16 shows the friction coefficient of the FSPed samples under varying sliding speed conditions. The results show that the substrate material had the highest friction coefficient among all the samples and its friction coefficient was around 0.53 to 0.64 when the speed increased from 1 m/s to 6 m/s. The FSPed recycled AA 6063/$TiO_2$ had a lower friction coefficient ranging from 0.27 to 0.53. Among all the FSPed samples, the samples produced at 2442 rpm with 50 mm/min, 1800 rpm with 45 mm/min, and 1200 rpm with 30 mm/min had relatively

low friction coefficients in varying nominal contact pressures, sliding speeds and sliding distances tests. As discussed above, the sample produced at 2442 rpm and 50 mm/min had the most homogeneous distribution of reinforcement particles and its surface microhardness was also consistent along the stir zone. Hence, the homogeneous distribution of the $TiO_2$ nano-powder (i.e., the sample produced at 2442 rpm, refer to Figure 13) and the consistent surface microhardness may have resulted in the lowest friction coefficient among all other samples.

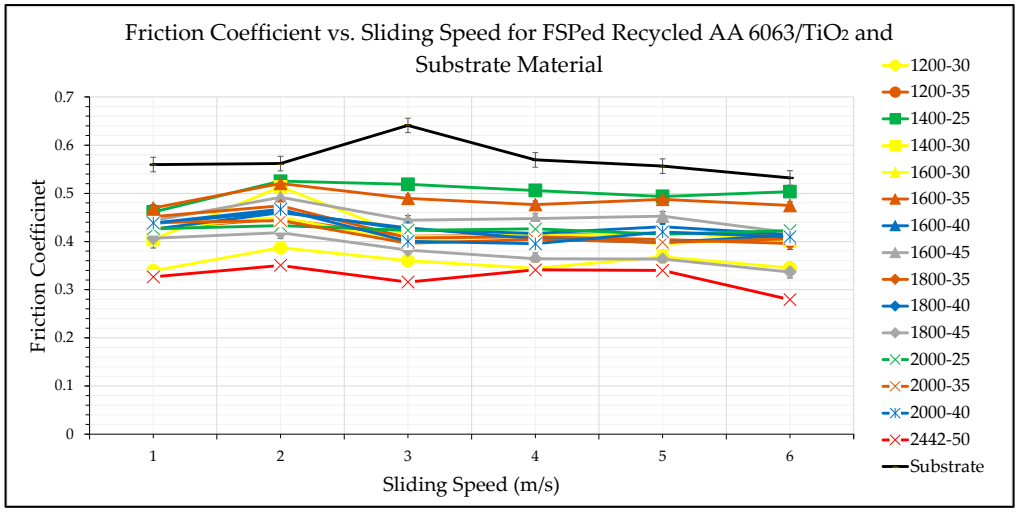


**Figure 16.** Friction coefficient against sliding speed for substrate material and FSPed samples subjected to a nominal contact pressure of 0.28 MPa for a test duration of 120 s under starved lubrication conditions.

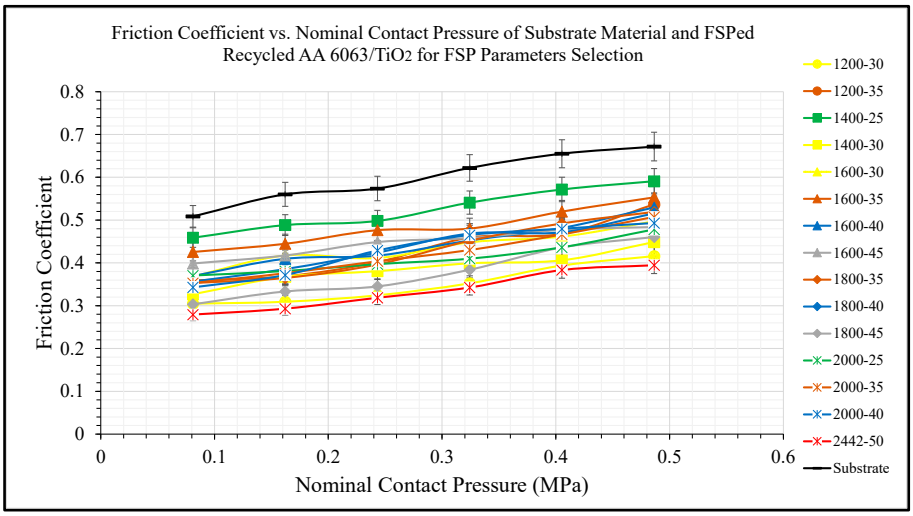


**Figure 17.** Friction coefficient against nominal contact pressure for substrate material and FSPed samples at a sliding speed of 5.18 m/s for a test duration of 120 s under starved lubrication conditions.

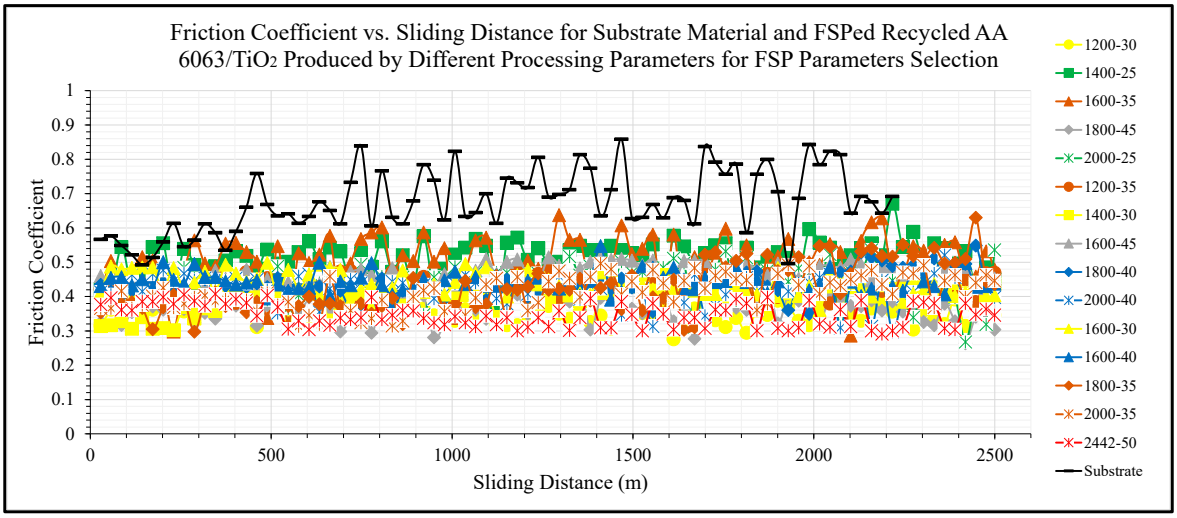


**Figure 18.** Sliding friction coefficient against sliding time of 2.5 km for substrate material and FSPed samples subjected to a nominal contact pressure of 0.24 MPa at a sliding speed of 2.88 m/s under starved lubrication conditions.

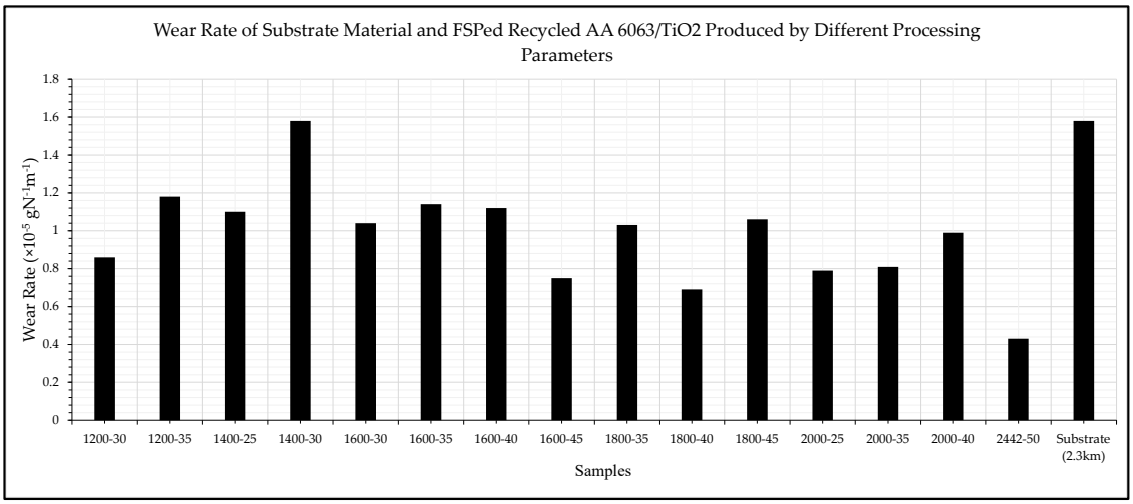


**Figure 19.** Wear rate for substrate material and FSPed samples after sliding for 2.5 km subjected to a nominal contact pressure of 0.24 MPa at a sliding speed of 2.88 m/s under starved lubrication conditions.

Next, Figure 17 presents the effects of nominal contact pressure on the friction coefficient of the substrate material and the FSPed samples. The results show that the friction coefficient of all the samples increased with the nominal contact pressure. This trend was also reported by Satyananda et al. [24]. Similar to the condition in varying sliding speed, the substrate material has the highest friction coefficient, which increased from 0.51 to 0.67 when the nominal contact pressure increased from 0.08 MPa to 0.47 Mpa. All the FSPed recycled AA 6063/$TiO_2$ has a similar friction coefficient because the amount of reinforced $TiO_2$ nano-powder was the same. However, the sample produced at 2442 rpm and 50 mm/min has the lowest friction coefficient, which increased from 0.28 to 0.39 when nominal contact pressure increased from 0.08 MPa to 0.47 MPa. This may have resulted from the homogeneous distribution of the $TiO_2$ nano-powder along the FSPed surface which led to a better surface microhardness.

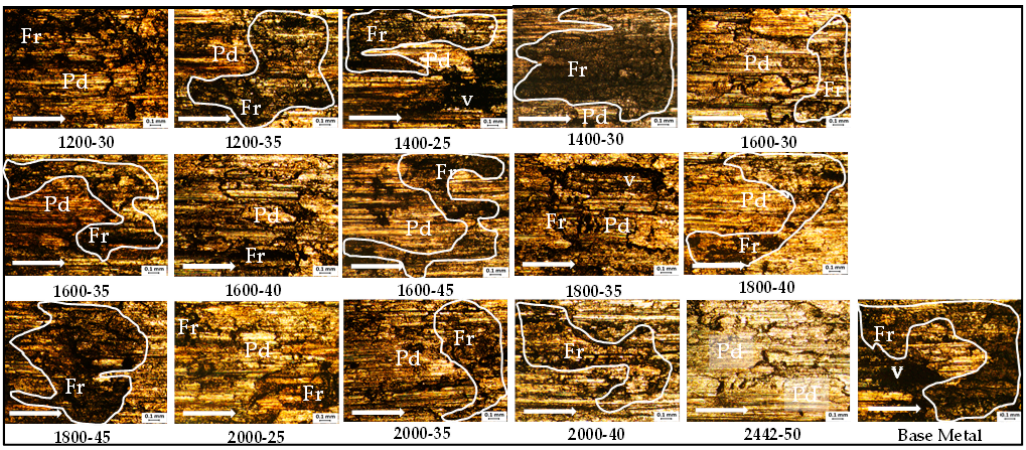


**Figure 20.** Wear morphology of substrate material and FSPed recycled AA 6063/$TiO_2$ produced by different processing parameters after 2.5 km of sliding distance test subject to a nominal contact pressure of 0.24 MPa at a sliding speed of 2.88 m/s under starved lubrication conditions. (Note: white arrow indicates sliding direction, V: voids, Fr: fractures, Pd: plastic deformation).

The substrate material and the FSPed samples were tested for a 2.5 km sliding test. The friction coefficient and their wear rate after the sliding test under starved lubrication conditions are presented in Figures 18 and 19. The friction coefficient of the substrate is the highest among all the FSPed recycled AA 6063/$TiO_2$ samples, Figure 18. All the FSPed samples show a similar trend of friction coefficients that ranged from 0.32 to 0.49. The sample produced at 2442 rpm and 50 mm/min exhibits the lowest friction coefficient. Meanwhile, the samples produced at 1200 rpm with 30 mm/min and 1800 rpm with 45 mm/min give relatively low friction coefficients but their wear rates are relatively high compared with the sample produced at 2442 rpm with 50 mm/min. Figure 19 shows that the unprocessed substrate material has the highest wear rate, $1.6 \times 10^{-5}$ $gN^{-1}m^{-1}$ and the samples produced at 2442 rpm and 50 mm/min has the smallest wear rate, $0.43 \times 10^{-5}$ $gN^{-1}m^{-1}$. The difference in friction coefficient may have been due to the non-uniform distribution of the $TiO_2$ nano-powder.

Figure 20 demonstrates the wear morphology of the substrate material and the FSPed samples after sliding for 2.5 km under starved lubrication conditions. Both abrasive and adhesive wear mechanisms can be observed from the wear morphology. The substrate material has a large portion of voids and fractures on the worn surface while most of the FSPed samples have plastic deformation and fractures with a small number of voids on the worn surfaces. The sample produced at 2442 rpm and 50 mm/min has the highest wear resistance and hence its worn surface was full of plastic deformation and no voids and fractures could be observed.

A comparison of the average friction coefficient of FSPed recycled AA 6063 from previous work [10] and the FSPed recycled AA 6063/$TiO_2$ is presented in Figure 21. The result shows that all the FSP samples experienced a reduction in friction coefficient. The FSPed recycled AA 6063/$TiO_2$ has a lower friction coefficient than the FSPed recycled AA 6063. This shows that the incorporation of $TiO_2$ powder successfully further reduced the friction coefficient of FSPed recycled AA 6063.

The friction and wear test results have shown that all the FSPed samples have friction reduction and it is further reduced after reinforcing with $TiO_2$. This shows that $TiO_2$ nano-powder can reduce the friction and wear of recycled AA 6063. This result also agreed with Heidarpour et al. [17], who used $TiO_2$ to enhance the tribological performance of copper. Their study also reported on the non-uniform distribution of $TiO_2$ not resulting in the best enhancement in surface microhardness and tribological performance [17]. This explains why the sample produced at 2442 rpm and 50 mm/min has the most uniform distribution of $TiO_2$ nano-powder, thereby resulting in the best tribological performance. The variation in

friction coefficient and wear rate of the FSPed samples produced by other processing parameters may be due to the non-uniform distribution of $TiO_2$ nano-powder. Grain refinement and enhancement in surface microhardness also reduced friction and wear of recycled AA 6063. Improvement in surface microhardness and grain refinement resulting in enhanced tribological properties is also reported by Yasavol et al. and Iswazko et al. [24–26].

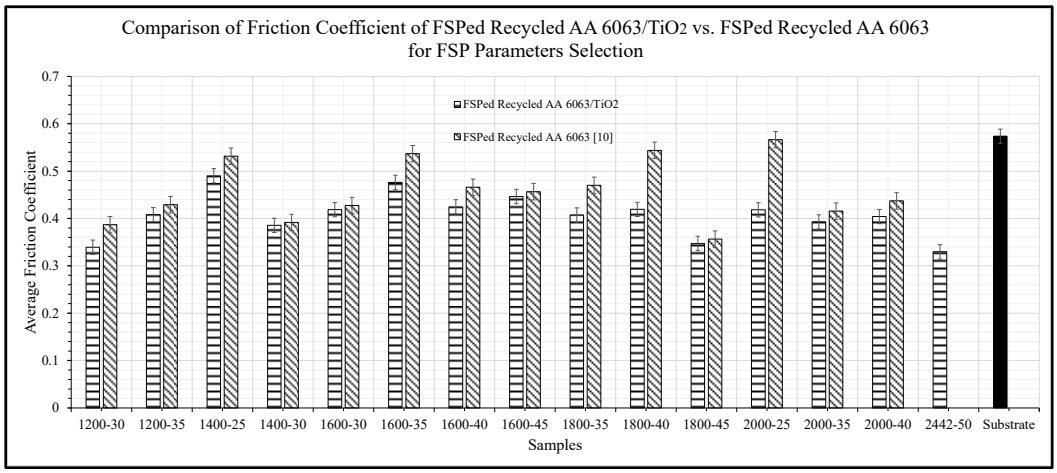


**Figure 21.** The comparison of the average friction coefficient of substrate material, FSPed recycled AA 6063 and FSPed recycled AA 6063/$TiO_2$ subjected to a nominal contact pressure of 0.24 MPa at a sliding speed of 2.88 m/s under starved lubrication conditions.

## 4. Conclusions

The objective of this study is to determine the best possible processing parameters for the fabrication of FSPed recycled AA 6063/$TiO_2$ by referring to its surface microhardness and tribological performance. This work can be concluded as below:

- The highest surface microhardness is achieved by the FSPed recycled AA6063/$TiO_2$ sample produced at 2442 rpm and 50 mm/min: 55.6 HV1. This surface microhardness is 16% higher than FSPed recycled AA 6063 and 45% higher than the substrate material.
- The microstructure of the FSPed recycled AA6063/$TiO_2$ sample that was produced at 2442 rpm and 50 mm/min exhibits the most uniform distribution of $TiO_2$ and it also achieves the greatest reduction of grain size.
- The FSPed recycled AA6063/$TiO_2$ sample produced at 1200 rpm with 30 mm/min, 1800 rpm with 45 mm/min and 2442 rpm with 50 mm/min give relatively low friction coefficients, while only the sample produced at 2442 rpm and 50 mm/min has the lowest friction coefficient and wear rate. This sample has an average friction coefficient of 0.33 and a wear rate of 0.43 $\times$ $10^{-5}$ $gN^{-1}m^{-1}$. This result reduced the friction coefficient and wear rate of the substrate by 39% and 73%, respectively.
- The wear morphology shows that both adhesive and abrasive wear can be observed. The FSPed samples have mostly plastic deformation with some fractures and a small number of voids. However, only plastic deformation can be observed in the sample produced at 2442 rpm and 50 mm/min.
- In short, the most suitable processing parameters used in this study for the fabrication of FSPed recycled AA 6063/$TiO_2$ are 2442 rpm and 50 mm/min. These parameters produced the sample with the highest surface microhardness, and lowest wear rate and friction coefficient. However, further study is needed to investigate the effect of rotational speeds and feed rates that are higher and lower than 2442 rpm and 50 mm/min for enhancing tribological performance of FSPed recycled AA 6063/$TiO_2$ surface composites.

**Author Contributions:** Conceptualization, K.W.L. and G.S.T.; Methodology, K.W.L. and G.S.T.; Formal analysis, K.W.L. and G.S.T.; Investigation, K.W.L., G.S.T. and C.K.K.; Resources, K.W.L.; Data curation, G.S.T.; Writing—original draft preparation, K.W.L. and G.S.T.; Writing—review and editing, K.W.L., C.K.K. and G.S.T.; Supervision, K.W.L.; Project administration, K.W.L.; Funding acquisition, K.W.L. and C.K.K. All authors have read and agreed to the published version of the manuscript.

**Funding:** This research was funded by Fundamental Research Grant Scheme, [FRGS/1/2019/TK03/MMU/02/6].

**Institutional Review Board Statement:** Not applicable.

**Informed Consent Statement:** Not applicable.

**Data Availability Statement:** Data available on request.

**Acknowledgments:** This work was supported by Fundamental Research Grant Scheme (FRGS), Ministry of Higher Education, Malaysia. The authors gratefully acknowledge EL Aluminium Billet Sdn. Bhd. for the technical and partial financial support rendered. Special thanks to the Faculty of Engineering and Technology of Multimedia University for their support in allowing this research to be carried out.

**Conflicts of Interest:** The authors declare no conflict of interest.

## References

1. Deamley, P.A.; Weiss, H. Energy conservation through surface engineering. *Tribol. Energy Conserv.* **1998**, *34*, 311–318.
2. Teo, G.S.; Liew, K.W.; Kok, C.K. Enhancement of Microhardness and Tribological Properties of Recycled AA 6063 Using Energy-Efficient and Environment-Friendly Friction Stir Processing. *IOP Conf. Ser. Earth Environ. Sci.* **2021**, *943*, 12–19. [CrossRef]
3. Sharma, V.; Prakash, U.; Manoj Kumar, B.V. Surface composites by friction stir processing: A review. *J. Mater. Process. Technol.* **2015**, *224*, 117–134. [CrossRef]
4. Weglowski, M.S.; Hamilton, C.B. An Experimental Investigation and Modelling of Friction Stir Processing. *Eng. Trans.* **2013**, *61*, 65–80.
5. Smith, C.B.; Harington, J.; Kouch, T. *Friction Stir Processing for Efficient Manufacturing*; Friction Stir Link, Inc.: Waukesha, WI, USA, 2012.
6. Lorenzo-Martin, C.; Ajayi, O.; Smith, C.; Krol, S. Energy efficient surface hardening of 4140 steel by friction stir processing for tribological applications. *Int. Jt. Tribol. Conf.* **2011**, *54747*, 63–65.
7. Gibsona, B.T.; Lammleinb, D.H.; Praterc, T.J.; Longhurstd, W.R.; Coxa, C.D.; Balluna, M.C.; Dharmaraja, K.J.; Cooka, G.E.; Straussa, A.M. Friction Stir Welding: Process, automation, and control. *J. Manuf. Process.* **2014**, *16*, 56–73. [CrossRef]
8. Lima, D.K.; Shibayanagib, T.; Gerlicha, A.P. Synthesis of multi-walled CNT reinforced aluminium alloy composite via friction stir processing. *Mater. Sci. Eng.* **2009**, *507*, 194–199. [CrossRef]
9. Har Moosbrugger, C. *Introduction to Magnesium Alloy. Engineering Properties of Magnesium Alloys*, 2nd ed.; Marken, K., Marquard, L., Eds.; ASM International: Materials Park, OH, USA, 2017; pp. 1–12.
10. Teo, G.S.; Liew, K.W.; Kok, C.K. Optimization of Friction Stir Processing Parameters of Recycled AA 6063 for Enhanced Surface Microhardness and Tribological Properties. *Metals* **2022**, *12*, 310. [CrossRef]
11. Shanmugasundaram, A.; Arul, S.; Sellamuthu, R. Investigating the Effect of WC on the Hardness and Wear Behavior of Surface Modified AA 6063. *Mater. Todays* **2018**, *5*, 6579–6587. [CrossRef]
12. Rathee, S.; Maheshwari, S.; Siddiquee, A.N.; Srivastava, M. Analysis of Microstructural Changes in Enhancement of Surface Properties in Sheet Forming of Al alloys via Friction Stir Processing. *Mater. Today Proc.* **2017**, *4*, 452–458. [CrossRef]
13. Srivastava, M.; Rathee, S.; Maheshwari, S.; Siddiquee, A.N. Optimization of Friction Stir Processing Parameters to Fabricate AA6063/SiC Surface Composites Using Taguchi Technique. *Int. J. Mater. Prod. Technol.* **2019**, *58*, 16–31. [CrossRef]
14. Murali, S.; Chockalingam, A.; Suresh Kumar, S.; Remanan, M. Production, Characterization and Friction Stir Processing of AA6063-T6/Al3Tip in-situ Composites. *Int. J. Mech. Prod.* **2018**, *2018*, 399–406.
15. Liang, X.; Cui, S.; Lia, H.; Abdelhady, A.; Wang, H.; Zhou, H. Removal effect on stormwater runoff pollution of porous concrete treated with nanometer titanium dioxide. *Transp. Res.* **2019**, *73*, 34–45. [CrossRef]
16. Skocaj, M.; Filipic, M.; Petkovic, J.; Novak, S. Titanium dioxide in our everyday life; Is it safe? *Radiol. Oncol.* **2011**, *45*, 227–247. [CrossRef] [PubMed]
17. Heidarpour, A.; Mazaheri, Y.; Roknian, M.; Ghasemi, S. Development of Cu-$TiO_2$ surface nanocomposite: Effect of pass number on microstructure, mechanical properties, tribological and corrosion behavior. *J. Alloys Compd.* **2019**, *783*, 886–897. [CrossRef]
18. Khodabakhshi, F.; Simchi, A.; Kokabi, A.H.; Gerlich, A.P.; Nosko, M. Effects of post-annealing on the microstructure and mechanical properties of friction stir processed Al–Mg–$TiO_2$ nanocomposites. *Mater. Des.* **2014**, *63*, 30–41. [CrossRef]
19. Abraham, S.J.; Dinaharan, I.; Selvam, J.D.R.; Akinlabi, E.T. Microstructural Characterization and Tensile Behavior of Rutile ($TiO_2$)-Reinforced AA6063 Aluminum Matrix Composites Prepared by Friction Stir Processing. *Acta Metall. Sin.* **2019**, *32*, 52–62. [CrossRef]

20. Sathiskumar, R.; Dinaharan, I.; Murugan, N.; Vijay, S.J. Influence of tool spindle speed on microstructure and sliding wear behavior of Cu/$B_4C$ surface composite synthesized by friction stir processing. *Trans. Nonferrous Met. Soc. China* **2015**, *25*, 95–102. [CrossRef]
21. Eskandari, H.; Taheri, R.; Khodabakhshi, F. Friction-stir processing of an AA8026-$TiB_2$-$Al_2O_3$ hybrid nanocomposite: Microstructural developments and mechanical properties. *Mater. Sci. Eng.* **2016**, *660*, 84–96. [CrossRef]
22. Qin, D.; Shen, H.; Shen, Z.; Chen, H.; Fu, L. Manufacture of biodegradable magnesium alloy by high speed friction stir processing. *J. Manuf. Process.* **2018**, *36*, 22–32. [CrossRef]
23. Zhang, Z.Y.; Yang, R.; Li, Y.; Chen, G.; Zhao, Y.T.; Liu, M.P. Microstructural evolution and mechanical properties of friction stir processed $ZrB_2$/6061Al nanocomposites. *J. Alloys Compd.* **2018**, *762*, 312–318. [CrossRef]
24. Kar, S.; Sahu, B.B.; Kousaka, H.; Han, J.G.; Hori, M. Study of the effect of normal load on friction coefficient and wear properties of $CN_x$ thin films. *AIP Adv.* **2020**, *10*, 1–9. [CrossRef]
25. Yasavol, N.; Ramalho, A. Wear properties of friction stir processed AISI D2 tool steel. *Tribol. Int.* **2015**, *91*, 177–183. [CrossRef]
26. Iwaszko, J.; Kuda, K.; Fila, K.; Strzelecka, M. The effect of friction stir processing (fsp) on the microstructure and properties of am60 magnesium alloy. *Arch. Metall. Mater.* **2016**, *61*, 1209–1214. [CrossRef]